ORIGINAL PAPER

CrossMark

Bacterial communities involved directly or indirectly in the anaerobic degradation of cellulose

Yuanyuan Bao[1,2] · Jan Dolfing[3] · Baozhan Wang[1] · Ruirui Chen[1] · Miansong Huang[4] · Zhongpei Li[1] · Xiangui Lin[1] · Youzhi Feng[1]

Abstract

To determine bacterial communities involved, directly or indirectly, in the anaerobic degradation of cellulose, we conducted a microcosm experiment with soil treated with ^{13}C-cellulose, ^{12}C-cellulose, or without cellulose with analyses of DNA-based stable isotope probing (DNA-SIP), real-time quantitative PCR, and high-throughput sequencing. Firmicutes, Actinobacteria, Verrucomicrobia, and Fibrobacteres were the dominant bacterial phyla-degrading cellulose. Generally, bacteria possessing gene-encoding enzymes involved in the degradation of cellulose and hemicellulose were stimulated. Phylotypes affiliated to *Geobacter* were also stimulated by cellulose, probably due to their role in electron transfer. Nitrogen-fixing bacteria were also detected, probably due to the decreased N availability during cellulose degradation. High-throughput sequencing showed the presence of bacteria not incorporating ^{13}C and probably involved in the priming effect caused by the addition of cellulose to soil. Collectively, our findings revealed that a more diverse microbial community than expected directly and indirectly participated in anaerobic cellulose degradation.

Keywords Cellulose degradation · Paddy soil · Cellulolytic bacteria · Syntrophic microorganisms · Nitrogen-fixing bacteria · Priming effect

Introduction

Annually, more than 7×10^{10} Mg of organic carbon (C) is produced by terrestrial plants globally (Paul and Clark 1989). Cellulose, which makes up 40–60% of the plant biomass, is the largest natural organic input to terrestrial ecosystems (Richmond 1991). Spatiotemporal degradation of cellulosic material to oligomers, to monomers, and to CO_2 and CH_4 is important for the genesis and development of soils and to nutrient cycling (Xiang et al. 2010).

Although most plant-derived cellulose is degraded under oxic conditions, about 5–10% is degraded under anoxic conditions, largely by bacteria (Pérez et al. 2002). Anaerobic fermentation and respiration of organic C are associated with the use of a diverse set of electron acceptors other than O_2 (Brune et al. 2000). The microbial processes involved in the anaerobic decomposition of cellulosic material are typically limited by electron acceptor availability. In the anoxic zone, when electron acceptors, such as Mn (IV), Fe (III), SO_4^{2-}, and CO_2, are exhausted, and cannot be effectively regenerated (Clément et al. 2005; Li et al. 2012a; Liesack et al. 2000), intermediate degradation products (e.g., alcohols and fatty acids) can accumulate and this impedes further degradation of polymer materials, unless syntrophic bacteria can establish syntrophic interactions with methanogens, guiding the removal of superfluous reducing equivalents. This can accelerate the catabolism of intermediate products and promote degradation of polymer materials (Liesack et al. 2000). Thus, anaerobic

✉ Youzhi Feng
yzfeng@issas.ac.cn

1 State Key Laboratory of Soil and Sustainable Agriculture, Institute of Soil Science, Chinese Academy of Sciences, Nanjing 210008, People's Republic of China

2 University of Chinese Academy of Sciences, Beijing 100049, People's Republic of China

3 School of Engineering, Newcastle University, Newcastle-upon-Tyne NE1 7RU, UK

4 Beijing Capital Co., LTD, Beijing 100028, People's Republic of China

decomposition of cellulose is associated with diverse syntrophic bacterial species. In addition, heterotrophic microorganisms usually have lower C:N ratios than the soils they inhabit (Bengtsson et al. 2003). Therefore, the microbial degradation of cellulose with a high C:N ratio can only occur if nitrogen (N)-fixing bacteria are also present. However, only a few studies have been conducted to identify the microbial species involved (Chatzinotas et al. 2013; Fan et al. 2014; Wegner and Liesack 2016), and these studies have generally been focused on the putative cellulose degraders. The associated microorganisms that also participate in anaerobic cellulose degradation and mineralization are poorly known.

Cellulose addition, the fresh organic matter (FOM), to soil accelerates soil organic matter (SOM) mineralization, that is, it causes the priming effect (Bingeman et al. 1953). Fontaine et al. (2003) suggested that the amendment of FOM, like cellulose, can firstly stimulate r-strategists and thus stimulate SOM decomposition rates, and then catabolites of SOM can stimulate K-strategists which further accelerate the degradation of SOM. Because of the biochemical similarities between FOM and SOM (Fontaine et al. 2004), we suggest that those r- and K-strategists may be involved in the anaerobic degradation and mineralization of cellulose. Despite the plethora of studies documenting responses of soil microorganisms to cellulose addition (Chatzinotas et al. 2013; Haichar et al. 2007; Nottingham et al. 2018), the microbial taxa stimulating the priming effect are not known and the relative mechanisms should be investigated. The above knowledge led us to hypothesize that, in addition to cellulolytic microorganisms also other, associated microorganisms are indirectly involved in the cellulose degradation process, and that these microorganisms are not necessarily labeled when labeled cellulose is added to the soil.

DNA-based stable isotope probing (DNA-SIP) can identify microorganisms involved in anaerobic breakdown of plant polymers (Li et al. 2011, 2012b). Apart from cellulolytic bacteria directly involved in cellulose degradation, DNA-SIP can also reveal some bacterial taxa utilizing intermediates of the cellulose degradation (Fan et al. 2014). Cross feeding (feeding on ^{13}C-intermediates derived from substrates) is one of the drawbacks of the DNA-SIP technique (Dumont et al. 2011), resulting in overestimation of label incorporation in DNA (Haichar et al. 2007). Intermediates are produced during the degradation of polymer materials under anoxic conditions (Rui et al. 2009). Identifying microbial taxa that utilize these intermediates could improve our understanding of microbes involved in cellulose degradation. Thus, this disadvantage of DNA-SIP can be turned into an advantage, if we identify these associated microorganisms.

The aim of this study was to identify soil bacterial species, including the associated species involved in the anaerobic degradation of cellulose in paddy soils. This was done by using ^{13}C-labeled cellulose and monitoring DNA-SIP in combination with high-throughput sequencing. We further performed real-time quantitative PCR (qPCR) to determine the abundances of labeled species in comparison with those whose DNA was amplified.

Materials and methods

Soil sample and pre-incubation

Soils for the microcosm experiment were sampled from Changshu agroecosystem experimental station, Jiangsu Province, China (31° 33′ N, 120° 42′ E). The main soil properties were 12.7% sand (0.05–2 mm); 63.6% silt (0.002–0.05 mm); 23.8% clay (< 0.002 mm); 1.14 g cm^{-3} bulk density; 12.6 g kg^{-1} soil organic C (SOC); 1.75 g kg^{-1} total N; 0.73 g kg^{-1} total P; and a pH of 6.6. Ten grams of paddy soil was added to serum bottles (120 ml, 10 cm in height) and pre-incubated for 3 days in a dark chamber at 27 °C.

^{13}C-labeled cellulose degradation experiment

After pre-incubation, 0.1 g of ^{13}C-labeled cellulose (98 at%, Cambridge Isotope Laboratories, Inc.) was added to each serum bottle (^{13}C), and the soil moisture was adjusted to 60% of maximum water holding capacity. The headspace of serum bottles was flushed with N$_2$ for 10 min, and then bottles were sealed and incubated in the dark at 27 °C for 13 days. Additionally, two parallel treatments were established for comparison (both were the control of the ^{13}C treatment): one concerned soils with added natural ^{12}C-cellulose (ca. 1.08% of ^{13}C to ΣC) amendment (^{12}C), and the other included soils without cellulose amendment (control). Both treated soils were incubated under the conditions reported above. Each treatment was replicated three times.

Gas samples were collected from the headspace of the soil microcosms at days 3, 6, 9, 12, and 13 with a gas-tight syringe. The concentrations of CO$_2$ and CH$_4$ were analyzed by gas chromatography with ECD (Agilent 7890A, Agilent Technologies). The evolved ^{13}C-CO$_2$ was analyzed by GC-IRMS using a pre-concentration unit (Thermo Finnigan Delta C+ and Precon, Thermo Finnigan, Bremen, Germany). On the day after final gas sampling, the soil of each serum bottle was sampled and stored at − 20 °C for DNA extraction and for the SIP experiment.

DNA extraction

Soil DNA was extracted from 0.5 g soil using the FastDNA® SPIN Kit (MP Biomedicals, Santa Ana, CA) including a negative control, as recent studies reported that kits and solutions may be contaminated with microbial DNA (Schöler et al. 2017; Vestergaard et al. 2017).

The extracted DNA was eluted in 50 µl of TE buffer, quantified by Nanodrop 2000 (ThermoFisher, USA) and stored at −20 °C before being analyzed.

Isopycnic centrifugation and gradient fractionation

Stable isotope fractionation was conducted as described by Jia and Conrad (2009) and Neufeld et al. (2007). Briefly, the gradient fractionation of total DNA extract (3.0 µg) from soil of all three SIP microcosms was performed with an initial CsCl buoyant density of 1.720 g/ml; the DNA was subjected to centrifugation at 177,000g for 44 h at 20 °C and then the buoyant density of each fraction (340 µl) was determined by the refractive index. Fifteen fractions were generated with buoyant densities ranging from 1.6988 to 1.7498 g/ml; nucleic acids were separated from CsCl by PEG 6000 precipitation and precipitates were subsequently dissolved in 30 µl of TE buffer.

Real-time quantitative PCR

Each extracted DNA sample and each DNA fraction taken from the fractionation gradient were analyzed for qPCR to determine abundances of bacterial 16S rRNA genes (primer set 519F and 907R) (Ruppel et al. 2007) and abundances of methanogenic archaeal 16S rRNA genes (primer set 1106F and 1378R) (Feng et al. 2013), *nifH* genes (primer set PolFI and AQER) (Wartiainen et al. 2008), Geobacteraceae (primer set Geo494F and Geo825R) (Yi et al. 2013), and *Methanosarcinaceae* (primer set Msc380F and Msc828R) (Smith et al. 2016). Standard curves were obtained using 10-fold serial dilutions of the linear *Escherichia coli*-derived vector plasmid pMD18-T (TaKaRa, Japan) containing a cloned target gene, using 10^2 to 10^7 gene copies µl^{-1}. The reactions were performed in a C1000™ Thermal Cycler equipped with a CFX96™ Real-Time System (Bio-Rad, USA). The 25-µl reaction mixture contained 12.5 µl of SYBR® Premix Ex Taq™ (TaKaRa, Japan), 0.5 µM each primer, 200 ng BSA µl^{-1}, and 1.0 µl of template containing approximately 2–9 ng DNA. A negative control was always run with water with the template instead of soil DNA extract. The qPCR program was 94 °C for 5 min, followed by 35 cycles of 94 °C for 30 s, 55 °C for 30 s, and 72 °C for 60 s, and a final extension and signal reading at 72 °C for 10 min. The specificity of the amplification products was confirmed by melting curve analysis, and the size of the amplified fragments was checked using a 1.5% agarose gel. qPCR was performed in triplicate, and amplification efficiencies of 97.4–104% were obtained, with R^2 values of 0.966–0.998.

High-throughput sequencing libraries preparing and data processing

"Light" (buoyant densities of 1.7285, 1.7246, and 1.7208 g/ml) and "heavy" (buoyant densities of 1.7434, 1.7399, and 1.7365 g/ml) bacterial DNA extracted from ^{13}C- and ^{12}C-cellulose-labeled microcosms and the control (without cellulose amendment) were subjected to high-throughput sequencing, after amplification by the primer set 515F and 907R (Feng et al. 2015). Briefly, the oligonucleotide sequences had a 5-bp barcode fused to the forward primer as barcode + forward primer. PCR was carried out in 50-µl reaction mixtures containing 4 µl (initial 2.5 mM each) of deoxynucleoside triphosphates, 2 µl (initial 10 mM each) of forward and reverse primers, 2 U of Taq DNA polymerase (0.4 µl; TaKaRa, Japan), and 1 µl containing 50 ng of genomic community DNA as a template. Thirty-five cycles (95 °C for 45 s, 56 °C for 45 s, and 72 °C for 60 s) were performed with a final extension at 72 °C for 7 min. The purified bar-coded PCR products from all samples were normalized in equimolar amounts, prepared using a TruSeq™ DNA Sample Prep LT Kit and sequenced using a MiSeq Reagent Kit v2 (500 cycles) following the manufacturer's protocols. Negative controls were included to determine the presence of contaminant DNA in the used kits and solutions (Schöler et al. 2017; Vestergaard et al. 2017). The sequences were deposited into the DDBJ database (accession no. DRA005968).

Raw sequence data were assembled with FLASH (Magoc and Salzberg 2011) and processed with the UPARSE algorithm (Edgar 2013). Primers were trimmed with cutadapt (Version 1.9.2) (Martin 2011). Then, sequences with average quality scores below 25 and lengths less than 300 bp were discarded, chimeras were filtered by UPARSE, and possible contaminants (e.g., PhiX and host DNA) were removed. Taxonomy was determined using the RDP classifier for bacteria (Wang et al. 2007) with a 97% similarity for operational taxonomic units (OTUs). In total, we obtained 2,273,005 bacterial 16S rRNA gene sequences, ranging from 6129 to 95,399 sequences per sample, with a median value of 40,487 sequences per sample. Since an even depth of sampling is required for beta (β) diversity comparisons (Shaw et al. 2008), samples were randomly rarified to obtain 6100 sequences per sample for downstream analysis. The Bray-Curtis distance was calculated for comparisons of taxonomical community composition and was visualized using non-metric multidimensional scaling (NMDS) plots.

Metagenomic library construction and sequencing

Heavy genomic DNA fractions of ^{13}C, ^{12}C-cellulose treatments were amplified by using a REPLI-g Single Cell (sc) Kit (#150345; Qiagen, Hilden, Germany) according to the manufacturer's protocol. DNA was fragmented to an average

size of approximately 300 bp using Covaris M220 (Gene Company Limited, China) for paired-end library construction. A paired-end library was prepared by using a TruSeq™ DNA Sample Prep Kit (Illumina, San Diego, CA, USA). Adapters containing the full complement of sequencing primer hybridization sites were ligated to the blunt-end fragments. Paired-end sequencing was performed on an Illumina HiSeq4000 platform (Illumina Inc., San Diego, CA, USA) at Majorbio Bio-Pharm Technology Co., Ltd. (Shanghai, China) using a HiSeq 3000/4000 PE Cluster Kit and HiSeq 3000/4000 SBS Kits according to the manufacturer's instructions (www. illumina.com).

Sequence quality control and gene-encoding enzymes involved in carbohydrate metabolism

The 3′ and 5′ ends were stripped using SeqPrep (https://github. com/jstjohn/SeqPrep). Low-quality reads (length < 50 bp or with a quality value < 20 or having N bases) were removed by Sickle (https://github.com/najoshi/sickle). The de Bruijn graph-based assembler SOAPdenovo (http://soap.genomics. org.cn, Version 1.06) was employed to assemble short reads. K-mers varying from 1/3 to 2/3 of read lengths were tested for each sample. Scaffolds with a length over 500 bp were retained for statistical tests; we evaluated the quality and quantity of scaffolds generated by each assembly and chose the best K-mer, which yielded the minimum scaffold number and the maximum value of N50 and N90, respectively. Then, scaffolds with a length over 500 bp were extracted and broken into contigs without gaps. These contigs were used for further gene prediction and annotation.

Carbohydrate-active enzyme (CAZyme) annotations were conducted using hmmscan (http://hmmer.janelia.org/search/ hmmscan) against the CAZy database V5.0 (http://www. cazy.org/) with an e-value cutoff of $1e^{-5}$.

Statistical analysis

Statistical analyses were conducted using the IBM Statistical Product and Service Solutions (SPSS) Statistics for Windows (Version 13). The data are expressed as means with standard deviation (SD), and different letters indicate significant differences between different samples. Mean separation among treatments was evaluated with one-way ANOVA followed by post hoc Tukey's HSD tests. Difference of $P < 0.05$ was considered significant. Permutational multivariate analysis of variance (PERMANOVA) (Anderson and Walsh 2013) was conducted to test the statistically significant differences among light and heavy DNA fractions of ^{13}C, ^{12}C-cellulose treatments and the control, using R software (Vegan package, Version 3.1.2). The heavy DNA fractions of ^{13}C-cellulose-amended microcosms compared with the corresponding DNA fractions of ^{12}C-labeled microcosms by Manhattan

plots, using edger and dplyr packages and drawn by gplots package in R (Version 3.1.2), according to Zgadzaj et al. (2016). The cellulose decomposers were defined as the positively responding OTUs above a threshold of significance (false discovery rate-corrected P values, $\alpha = 0.05$) by comparing heavy DNA fractions of ^{13}C-cellulose-amended microcosms with the corresponding DNA fractions of ^{12}C-cellulose microcosms. The same method was used to analyze the responders in light DNA fractions of ^{13}C-cellulose-amended microcosms compared with the corresponding DNA fractions in control microcosms; the positively responding OTUs were defined as SOM decomposers.

Results

Carbon dioxide and methane evolution in the isotope-labeled microcosms

Both CO_2 and CH_4 concentrations in the headspace were monitored to determine microbial activity during the 13-day incubation period. In the cellulose treatments, CO_2 production reached a maximum ranging from 0.74 to 0.80 g C kg^{-1} dry weight soil (d.w.s) and the maximum CH_4 production ranged from 0.25 to 0.30 g C kg^{-1} d.w.s; both were significantly higher than in the controls without cellulose at all times ($P < 0.05$) (Fig. 1). The ^{13}C-atom abundance reached a maximum of approximately 78.9% (Fig. S1). The percentages of CO_2 derived from cellulose, SOM, and bulk soil at day 13 were 80.5%, 4.3%, and 15.3%, respectively (Fig. S2).

Shifts in the bacterial community composition of the isotopically fractionated DNA gradients

Real-time quantitative PCR revealed that the abundances of bacterial 16S rRNA genes (Fig. 2) were largely significantly higher in the heavy DNA fractions (i.e., buoyant densities of 1.7434, 1.7399, 1.7365, 1.7327, 1.7285, and 1.7246 g/ml) from the ^{13}C-cellulose-labeled treatment than in those from the control treatments (^{12}C-cellulose and control without cellulose amendment) at day 13 ($P < 0.05$).

The NMDS plot (Fig. 3) and permutation test based on Bray-Curtis distance (Table S1) revealed that the bacterial community compositions were significantly different between heavy and light DNA fractions of ^{13}C-cellulose-labeled soils and between heavy or light DNA fractions of two control (^{12}C-cellulose and without cellulose) treatments. Furthermore, no difference in community composition was observed for heavy DNA fractions between two controls. The above mentioned pattern again confirms that specific bacteria had metabolized ^{13}C-cellulose and assimilated its ^{13}C.
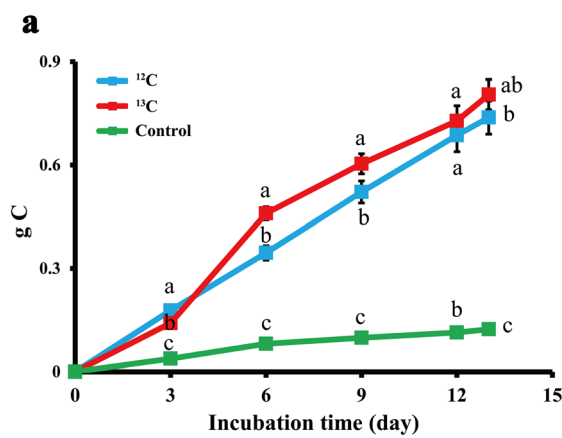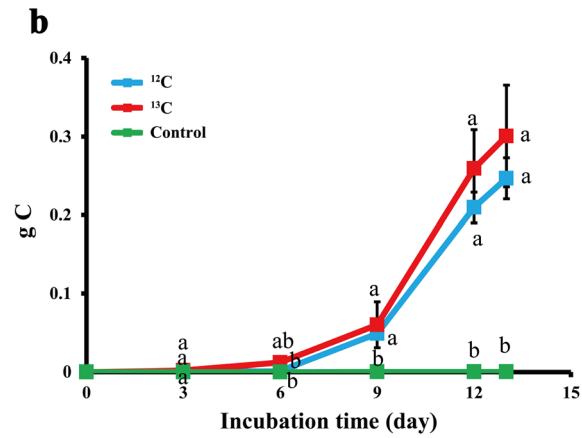
Fig. 1 CO_2 (**a**) and CH_4 (**b**) evolution in soil microcosms during incubation for 13 days. ^{13}C and ^{12}C denote the soil treated with ^{13}C- and ^{12}C-cellulose, respectively. Control is the treatment without cellulose addition. Standard error bars were obtained considering data of three replicates. The different letters above error bars indicate significant difference ($P < 0.05$)

Taxonomic distribution of the bacterial communities in heavy and light DNA fractions

In the heavy DNA fractions extracted from the microcosms treated with ^{12}C-cellulose, 79.2% of the sequences belonged to five bacterial phyla: Proteobacteria (32.9%), Acidobacteria (17.7%), Bacteroidetes (10.4%), Chloroflexi (10.3%), and Planctomycetes (7.9%) (Fig. 4). Similarly, the five dominant bacterial phyla of the heavy DNA fractions extracted from the non-amended controls were the Proteobacteria (35%), Acidobacteria (17.3%), Bacteroidetes (9.2%), Chloroflexi (9%), and Planctomycetes (8.1%). In the heavy DNA fractions extracted from the microcosms treated with ^{13}C-cellulose, Firmicutes was the most abundant phylum (36.6%), followed by Proteobacteria (26.7%), Acidobacteria (8%), and Actinobacteria (4%). Compared to the heavy DNA fractions treated with ^{12}C-cellulose, abundances of

Firmicutes, Actinobacteria, Verrucomicrobia, and Fibrobacteres were the most increased phyla in the heavy DNA fractions treated with ^{13}C-cellulose, while they exhibited lower relative abundances in the control. While these phyla collectively accounted for 45.8% of the heavy DNA fractions treated with ^{13}C-cellulose, they contributed only 9.8% of heavy DNA fractions extracted from control soil (Fig. 4).

We further compared the OTUs of heavy DNA fractions from soil samples treated with ^{13}C-cellulose and those of heavy DNA fractions from ^{12}C-cellulose-amended soils and found that there were 141 OTUs of cellulose decomposers, accounting for 2.3% of total OTUs in heavy fractions (Fig. 5a). These OTUs belonged to Firmicutes, accounting for 34.1% of total sequences in heavy fractions, followed by Proteobacteria (11.3%), Actinobacteria (3.7%), Verrucomicrobia (2.1%), and Fibrobacteres (0.6%) (Fig. 5b). They were assigned to three orders: Myxococcales (2.3%),
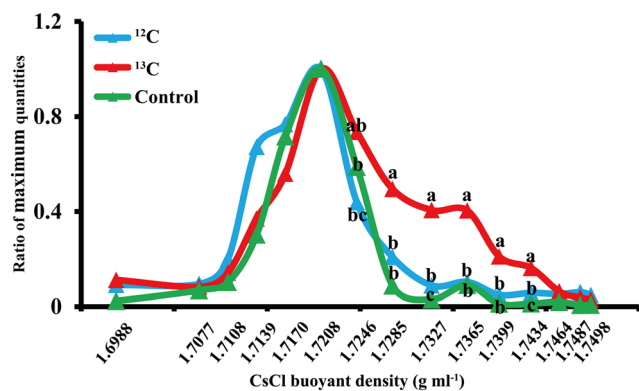

Fig. 2 Distributions of the copy numbers of bacterial 16S rRNA gene across the buoyant densities of the DNA gradients isolated from soil samples treated with ^{13}C- or with ^{12}C-cellulose or the untreated control. Values not followed by the same letter indicate a significant difference ($P < 0.05$) in the ratio of maximum quantities
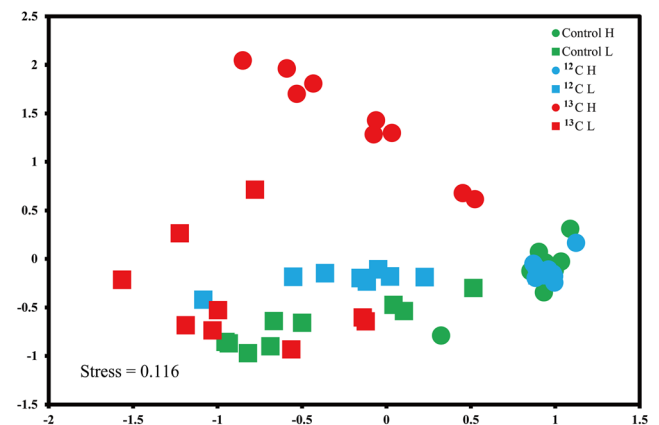

Fig. 3 Non-metric multidimensional scaling (NMDS) plots of changes in the Bray-Curtis distance calculated by considering community compositions of "heavy" and "light" DNA fractions extracted from soil samples treated with ^{13}C- or ^{12}C-cellulose or from the untreated control after incubation for 13 days

Fig. 4 The 100% stacked column chart of relative abundances of the dominant bacterial phylotypes in "heavy" and "light" DNA fractions in soil samples treated with ^{13}C- or ^{12}C-cellulose or the untreated control. The value of each phylum percentage is the mean of data from three replicates
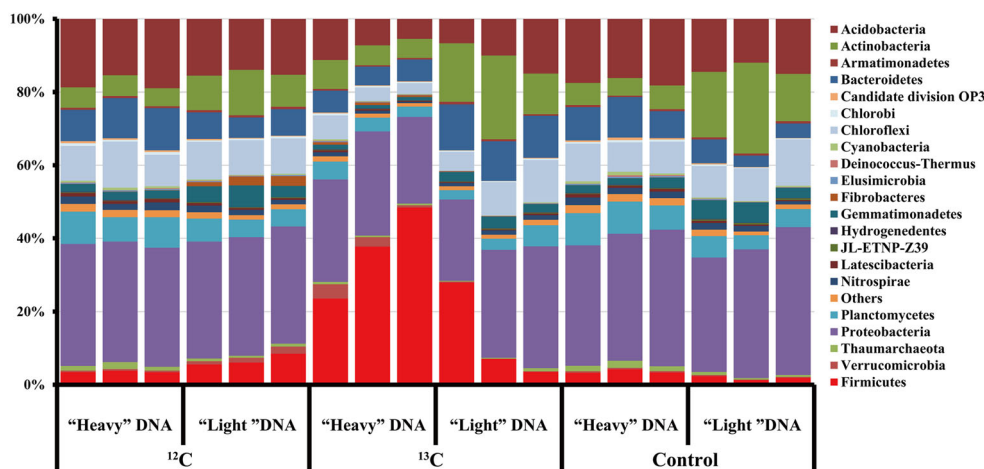
Fibrobacterales (0.6%), and Rhizobiales (0.1%); five families: Ruminococcaceae (15.5%), Lachnospiraceae (6.5%), Coriobacteriaceae (2.0%), Cellulosimicrobium (1.5%), and Opitutaceae (2.1%); and three genera: *Paenibacillus* (6.9%), *Geobacter* (5.9%), and *Pleomorphomonas* (0.1%) (Fig. 5c). Compared to the OTUs of light DNA fractions from soil samples treated without cellulose (control), there were 72 OTUs of SOM decomposers from light DNA fractions of ^{13}C-cellulose-amended soils. These OTUs belonged to Firmicutes, accounting for 10.7% of total sequences in light fractions, followed by Bacteroidetes (9.1%), Actinobacteria (0.9%), etc. They were assigned to three families: Ruminococcaceae

(2.5%), Clostridiaceae 1 (2.0%), and Lachnospiraceae (1.8%); and to four genera: *Mobilitalea* (1.3%), *Ruminiclostridium* (1.0%), *Flavisolibacter* (7.8%), and *Arthrobacter* (0.7%) (Table 1).

Comparative metagenomic analysis of CAZyme gene expression

Considerable differences in the CAZyme-encoding genes were observed comparing the heavy DNA fractions of soil samples treated with ^{13}C- and ^{12}C-cellulose. The number of CAZyme-encoding genes in the heavy DNA fractions in soil
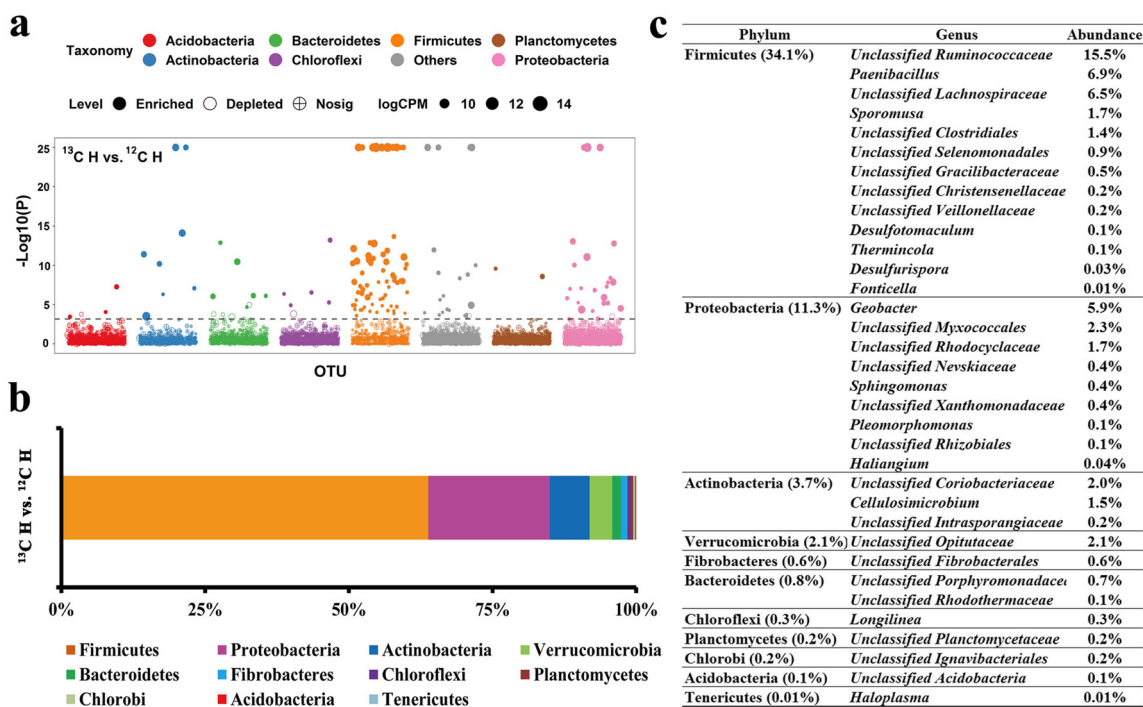

Fig. 5 Solid circles in Manhattan plots represent the OTUs (responders) of the "heavy" DNA fractions of ^{13}C-cellulose treatments, compared to ^{12}C-cellulose treatments (**a**). The dashed line indicates the significance threshold defined as a false discovery rate-corrected P value of 0.05 for the test. Dots above dashed line indicate significant difference ($P < 0.05$). The 100% stacked column chart shows the relative abundances of dominant responders (**b**). The detailed taxonomic information of responders (**c**)

Table 1 SOM-assimilating bacteria activated by the addition of cellulose

Phylum	Genus	Abundance (%)
Firmicutes (10.7%)	*Unclassified Ruminococcaceae*	2.5
	Unclassified Clostridiaceae 1	2.0
	Unclassified Lachnospiraceae	1.8
	Mobilitalea	1.3
	Ruminiclostridium	1.0
	Sporomusa	0.4
	Bacillus	0.3
	Paenibacillus	0.2
	Thermincola	0.2
	Oxobacter	0.1
	Desulfotomaculum	0.1
	Unclassified Clostridiales	0.1
	Unclassified Veillonellaceae	0.1
	Unclassified Peptococcaceae	0.1
	Unclassified Gracilibacteraceae	0.1
	Unclassified Selenomonadales	0.1
	Desulfosporosinus	0.1
	Clostridium sensu stricto 1	0.04
	Desulfitobacterium	0.04
	Sedimentibacter	0.04
	Proteiniclasticum	0.03
	Desulfurispora	0.03
	Unclassified Clostridiales	0.03
	Christensenellaceae R-7 group	0.03
Bacteroidetes (9.1%)	*Flavisolibacter*	7.8
	Unclassified Draconibacteriaceae	0.6
	Unclassified WCHB1-32	0.3
	Unclassified Bacteroidetes	0.2
	Unclassified Porphyromonadaceae	0.1
	Unclassified SB-5	0.1
Actinobacteria (0.9%)	*Arthrobacter*	0.7
	Unclassified Coriobacteriaceae	0.2
Armatimonadetes (0.1%)	*Unclassified Armatimonadetes*	0.1
Chlorobi (0.1%)	*Unclassified Ignavibacteriales*	0.1
Chloroflexi (0.03%)	*Longilinea*	0.03

samples treated with ^{13}C- and ^{12}C-cellulose was 1,367,092 and 2,238,266, respectively. These genes encoded (i) auxiliary activities (AAs), (ii) carbohydrate-binding modules (CBMs), (iii) carbohydrate esterases (CEs), (iv) glycoside hydrolases (GHs), (v) glycosyl transferases (GTs), and (vi) polysaccharide lyases (PLs). The gene-encoding PLs and CEs were increased in the heavy DNA fractions of soil treated with ^{13}C-cellulose compared to the heavy DNA fractions of soil treated with ^{12}C-cellulose (Fig. 6a). The number of CAZyme genes associated with "cellulose metabolic processes" in the heavy DNA fractions extracted from microcosms treated with ^{13}C-cellulose was increased compared to those of the extract from the microcosm treated with ^{12}C-cellulose (Fig. 6b). Gene-

encoding enzymes involved in chitin degradation were likely due to the presence of fungi in soil (Choi 2003).

The copy number of microbes stimulated by adding cellulose and their labeling in the heavy DNA fractions

After adding cellulose, the copy numbers of total bacteria, *Methanosarcinaceae*, Geobacteraceae, and *nifH* gene increased by 42.2%, 13.2%, 26.6%, and 4.6%, respectively, compared to the control without cellulose. However, only 73.0%, 4.0%, 5.0%, and 0.6% of these increased groups were labeled (Tables 2 and S2).
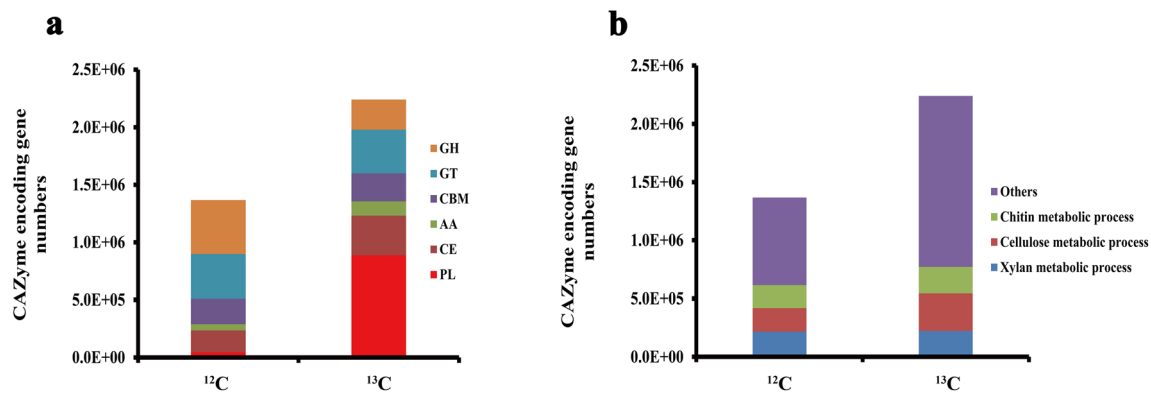
a

b

Fig. 6 Comparative metagenomic analyses of CAZyme gene expression in "heavy" DNA fractions of soil samples treated with ^{13}C- or with ^{12}C-cellulose. The genes are annotated to the microbiological processes indicated, whereas "others" means that genes cannot be annotated to biological processes involved in "xylan metabolism," "cellulose metabolism," and "chitin metabolism." Abbreviations: AAs, auxiliary activities; CBMs, carbohydrate-binding modules; CEs, carbohydrate esterases; GHs, glycoside hydrolases; GTs, glycosyl transferases; PLs, polysaccharide lyases

Discussion

Putative cellulolytic bacteria involved in cellulose degradation

In this study, DNA-SIP was used to identify microbial species responsible for cellulose degradation in a paddy soil incubated under anoxic conditions for 13 days. The bacterial community-degrading cellulose was dominated by the following phyla: Firmicutes, Actinobacteria, Verrucomicrobia, and Fibrobacteres (Fig. 4). Usually, these phyla are dominant during decomposition of plant residues (Bernard et al. 2007; España et al. 2011; Li et al. 2014; Liesack et al. 2000). At the high resolution, sequences of the heavy DNA fractions extracted from microcosms treated with ^{13}C-cellulose were related to cellulolytic bacteria of the order Myxococcales (2.3%), the families Ruminococcaceae (15.5%) and Lachnospiraceae (6.5%), and the genus *Paenibacillus* (6.9%) (Fig. 5c). These bacteria possess gene-encoding plant cell wall-degrading enzymes and can metabolize hemicellulose and/or cellulose (Flint et al. 2012; Miron and Ben-Ghedalia 1992; Moon et al. 2011; Ozbayram et al. 2017; Reichenbach et al. 2006). In addition, members having gene-encoding CAZymes are involved in the cleavage of glycosidic bonds present in xylan and cellulose (Coutinho et al. 2009). The number of gene-encoding CAZyme was higher in the heavy DNA fractions of the ^{13}C-cellulose-labeled treatment than in that of the ^{12}C-cellulose-labeled treatment at day 13 (Fig. 6a), thus indicating an increase of genes involved in xylan and cellulose degradation. According to Wegner and Liesack (2016), the phyla of Firmicutes, Actinobacteria, and Verrucomicrobia contribute to cellulose degradation by the expression of gene-encoding CAZymes. Therefore, the increase in the number of genes annotated to "cellulose metabolic processes" was due to the increase in abundances of phyla, Firmicutes, Actinobacteria, and Verrucomicrobia, in the heavy DNA fractions of the ^{13}C-cellulose-labeled treatment (Fig. 6b).

Although 13 days of incubation might not long enough for microbes to completely degrade cellulose, we chose this relatively short incubation period because the degrading microbial community was actively metabolizing cellulose. A longer incubation period would have increased the cross-feeding effect of the DNA-SIP technique resulting in labeling of microorganisms involved in the use of products of cellulose degradation. As shown in Figs. 1 and S2, the evolved gases suggest that the addition of cellulose stimulated microbial metabolism in the anoxic paddy soil. It has been reported that DNA-SIP detected labeled bacteria 7 days after adding cellulose and that the labeled populations were stable from days 14 to 30 (Bernard et al. 2007; Haichar et al. 2007). Therefore, 13 days of incubation were long enough to identify microbial species involved in cellulose degradation in this study.

Table 2 The percentage of total microbes present as target microbes stimulate by adding cellulose and the percentage of copy number of increased copy number stimulated by cellulose present in the "heavy" DNA fraction

	Total bacteria (%)	*Methanosarcinaceae* (%)	Geobacteraceae (%)	*nifH* (%)
Copy number increase percentage	44.2	13.2	26.6	4.6
^{13}C-labeling percentage	73.0	4.0	5.0	0.6

Syntrophic microorganisms involved in cellulose degradation

In addition to the observation of putative cellulolytic bacteria, stimulation of *Geobacter* was shown by the DNA-SIP technique (Fig. 5c). *Geobacter* species are involved in the dissimilatory iron reduction and prevail over methanogens in the presence of oxidized iron species such as ferrihydrite (Hori et al. 2010). *Geobacter* spp. can establish syntrophic interactions with methanogenic archaea via conductive pili or conductive materials, such as hematite and magnetite (Rotaru et al. 2014; Shrestha et al. 2013). These conductive materials act as the electrical conduit between the electron-donating *Geobacter* spp. and the electron-accepting methanogenic archaea, which is known as direct interspecies electron transfer (DIET). DIET can promote methanogenesis through interactions between methanogenic archaea and *Geobacter* spp. (Kato et al. 2012; Li et al. 2015). The stimulation of methanogenesis can remove reducing equivalents, thus enhancing organic matter degradation (Luo et al. 2016; Zhuang et al. 2015). Phylotypes affiliated to *Geobacter* and *Methanosarcinaceae* were observed in the heavy DNA fraction of ^{13}C-labeled microcosms by the metagenomic analyses (data not shown), suggesting that probably DIET occurred during cellulose degradation in the paddy soil. Wegner and Liesack (2016) reported the dominance of Geobacteraceae and *Methanosarcinaceae* in straw-amended soils after 7 and 14 days. Syntrophic communities of *Geobacter* and methanogenic archaea can utilize C from cellulose to efficiently remove reducing equivalents via DIET and can have an important role in the anaerobic cellulose degradation.

N-fixing microbes involved in cellulose degradation

The presence of N-fixing microbes, such as *Pleomorphomonas* and Rhizobiales (Fig. 5c), is likely the result of the decreased N availability and subsequent demands for N during the microbial-driven cellulose degradation. N immobilization generally occurs when the C:N ratio is ≥ 45 (Seneviratne 2000). In our study, the C:N ratio of cellulose was > 45, indicating that N availability was a limiting factor for the degradation of cellulose. This is similar to the reduction in N-trace gas emissions observed after the addition of cereal straw with high C:N ratios (Huang et al. 2004; Shan and Yan 2013) and similar to the presence of N-fixing microbes during the maize residue decomposition (Fan et al. 2014). Furthermore, Akiyama and Tsuruta (2003) reported a negative linear correlation between the magnitude of NO emissions from organic material-amended soils and the C:N ratio of the incorporated organic materials. In general, soil mineral N (NH_4^+ and NO_3^-) availability decreases by increasing C:N ratio of organic material due to heterotrophic microbial growth associated with N assimilation and there is a negative correlation between N-trace gas emissions and C:N ratios (Millar and Baggs 2005). For this reason, the microbial community needs N-fixing microbes to increase N availability, especially for cellulosic material degradation.

Addition of cellulose changed microbial composition which triggered apparent priming effect

qPCR results demonstrated that only a small number of the target microbes were labeled despite their relatively high increase in copy numbers after cellulose addition (Tables 2 and S2). The reason behind this phenomenon could be due to the priming effect (Fig. S2) (Bingeman et al. 1953) and to the shortcomings of the DNA-SIP technique (Neufeld et al. 2007). The addition of organic compounds to soil accelerates SOM mineralization by stimulating SOM decomposer populations and promoting SOM-decomposing enzyme activities (Fontaine et al. 2003). Probably the increased abundance of some microbial species caused the priming effect and such increase was due to cellulose degradation. Thus, we suggest that the non-labeled organisms (Geobacters and N-fixing microbes (Table 2)) triggered the priming effect and stimulated the decomposition of SOM (Fig. S2), and probably another 27% of unlabeled total bacteria (Table 2), including three bacterial families (Ruminococcaceae, Clostridiaceae 1, and Lachnospiraceae), and four bacterial genera (*Mobilitalea*, *Ruminiclostridium*, *Flavisolibacter*, and *Arthrobacter*) (Table 1), also triggered the priming effect. Extracellular SOM-decomposing enzymes are considered to accelerate FOM decomposition (Saiz-Jimenez 1996). Since those organisms were not labeled and some of them belonged to Firmicutes, which are usually dominant during plant residue decomposition (Li et al. 2014), we suggest that they can play an accessory role in the degradation of cellulose. These unlabeled taxa likely grew using soil organic compounds other than cellulose, and may co-exist synergistically with the putative cellulose-degrading bacteria. Non-labeled organisms are important in environmental processes. For example, Sun et al. (2017) used the DNA-SIP technique to monitor acetate- and lactate-oxidizing bacteria in anaerobic digester sludge, and constructed a co-occurrence network to show that microbes not enriched in the ^{13}C-DNA fractions also play an important role in anaerobic digestion.

Clearly, substantial DNA synthesis and cell division are required to incorporate sufficient label into DNA for subsequent gradient separation by the DNA-SIP technique. Increasing the number of cell divisions increases the extraction yield of labeled nucleic acid. The DNA-SIP technique generally identifies the most labeled microorganisms. Microorganisms that utilize mixed C sources, or grow relatively slowly will be poorly labeled and thus underestimated, even though they may have also contributed to cellulose degradation. These shortcomings of the DNA-SIP technique

could partly explain why cellulose amendment stimulated a vast community, while many of the community members did not incorporate ^{13}C from the labeled cellulose.

Conclusions

In this investigation, we identified different bacterial groups involved in the anaerobic decomposition of cellulose by using the DNA-SIP technique combined with qPCR in a laboratory microcosm experiment. As expected, the classical cellulose degraders predominated in DNA-SIP analyses. However, we also observed an increased presence of associated syntrophic bacteria such as those of the genus *Geobacter*, capable of reducing iron, and of N-fixing microbes, only part of which were probably directly involved in cellulose degradation. In addition, the abundance of species not enriched in ^{13}C-DNA fractions also increased upon addition of labeled cellulose, suggesting that they may also play a role in cellulose degradation, either directly or indirectly. These results suggest that the anaerobic degradation of plant residues involves more microbial groups than commonly expected. Future research should also consider these associated consortia for a better understanding of cellulose anaerobic degradation.

Publisher's note Springer Nature remains neutral with regard to jurisdictional claims in published maps and institutional affiliations.

References

Akiyama H, Tsuruta H (2003) Effect of organic matter application on N_2O, NO, and NO_2 fluxes from an Andisol field. Global Biogeochem Cy 17:1100

Anderson MJ, Walsh DCI (2013) PERMANOVA, ANOSIM, and the Mantel test in the face of heterogeneous dispersions: what null hypothesis are you testing? Ecol Monogr 83:557–574

Bengtsson G, Bengtson P, Mansson KF (2003) Gross nitrogen mineralization-, immobilization-, and nitrification rates as a function of soil C/N ratio and microbial activity. Soil Biol Biochem 35:143–154

Bernard L, Mougel C, Maron PA, Nowak V, Lévêque J, Henault C, Haichar FZ, Berge O, Marol C, Balesdent J (2007) Dynamics and identification of soil microbial populations actively assimilating carbon from ^{13}C-labelled wheat residue as estimated by DNA- and RNA-SIP techniques. Environ Microbiol 9:752–764

Bingeman CW, Varner JE, Martin WP (1953) The effect of the addition of organic materials on the decomposition of an organic soil. Soil Sci Soc Am J 17:34–38

Brune A, Frenzel P, Cypionka H (2000) Life at the oxic-anoxic interface: microbial activities and adaptations. FEMS Microbiol Rev 24:691–710

Chatzinotas A, Schellenberger S, Glaser K, Kolb S (2013) Assimilation of cellulose-derived carbon by microeukaryotes in oxic and anoxic slurries of an aerated soil. Appl Environ Microb 79:5777–5781

Choi SY (2003) Distribution of alcohol-tolerant microfungi in paddy field soils. Mycobiology 31:191–195

Clément JC, Shrestha J, Ehrenfeld JG, Jaffé PR (2005) Ammonium oxidation coupled to dissimilatory reduction of iron under anaerobic conditions in wetland soils. Soil Biol Biochem 37:2323–2328

Coutinho PM, Andersen MR, Kolenova K, Vankuyk PA, Benoit I, Gruben BS, Trejoaguilar B, Visser H, Van SP, Pakula T (2009) Post-genomic insights into the plant polysaccharide degradation potential of *Aspergillus nidulans* and and *Aspergillus oryzae*. Fungal Genet Biol 46:S161–S169

Dumont MG, Pommerenke B, Casper P, Conrad R (2011) DNA-, rRNA- and mRNA-based stable isotope probing of aerobic methanotrophs in lake sediment. Environ Microbiol 13:1153–1167

Edgar RC (2013) UPARSE: highly accurate OTU sequences from microbial amplicon reads. Nat Methods 10:996–998

España M, Rasche F, Kandeler E, Brune T, Rodriguez B, Bending GD, Cadisch G (2011) Identification of active bacteria involved in decomposition of complex maize and soybean residues in a tropical Vertisol using ^{15}N-DNA stable isotope probing. Pedobiologia 54:187–193

Fan F, Yin C, Tang Y, Li Z, Song A, Wakelin SA, Zou J, Liang Y (2014) Probing potential microbial coupling of carbon and nitrogen cycling during decomposition of maize residue by ^{13}C-DNA-SIP. Soil Biol Biochem 70:12–21

Feng Y, Lin X, Yu Y, Zhang H, Chu H, Zhu J (2013) Elevated ground-level O_3 negatively influences paddy methanogenic archaeal community. Sci Rep 3:3193

Feng YZ, Chen RR, Hu JL, Zhao F, Wang JH, Chu HY, Zhang JB, Dolfing J, Lin XG (2015) *Bacillus asahii* comes to the fore in organic manure fertilized alkaline soils. Soil Biol Biochem 81:186–194

Flint HJ, Scott KP, Duncan SH, Louis P, Forano E (2012) Microbial degradation of complex carbohydrates in the gut. Gut Microbes 3:289–306

Fontaine S, Mariotti A, Abbadie L (2003) The priming effect of organic matter: a question of microbial competition? Soil Biol Biochem 35:837–843

Fontaine S, Bardoux G, Benest D, Verdier B, Mariotti A, Abbadie L (2004) Mechanisms of the priming effect in a savannah soil amended with cellulose. Soil Sci Soc Am J 68:125–131

Haichar FEZ, Achouak W, Christen R, Heulin T, Marol C, Marais MF, Mougel C, Ranjard L, Balesdent J, Berge O (2007) Identification of cellulolytic bacteria in soil by stable isotope probing. Environ Microbiol 9:625–634

Hori T, Muller A, Igarashi Y, Conrad R, Friedrich MW (2010) Identification of iron-reducing microorganisms in anoxic rice paddy soil by ^{13}C-acetate probing. ISME J 4:267–278

Huang Y, Zou J, Zheng X, Wang Y, Xu X (2004) Nitrous oxide emissions as influenced by amendment of plant residues with different C:N ratios. Soil Biol Biochem 36:973–981

Jia ZJ, Conrad R (2009) Bacteria rather than Archaea dominate microbial ammonia oxidation in an agricultural soil. Environ Microbiol 11:1658–1671

Kato S, Hashimoto K, Watanabe K (2012) Methanogenesis facilitated by electric syntrophy via (semi)conductive iron-oxide minerals. Environ Microbiol 14:1646–1654

Li Y, Lee CG, Watanabe T, Murase J, Asakawa S, Kimura M (2011) Identification of microbial communities that assimilate substrate from root cap cells in an aerobic soil using a DNA-SIP approach. Soil Biol Biochem 43:1928–1935

Li Y, Yu S, Strong J, Wang H (2012a) Are the biogeochemical cycles of carbon, nitrogen, sulfur, and phosphorus driven by the "Fe^{III}-Fe^{II} redox wheel" in dynamic redox environments? J Soils Sediments 12:683–693

Li Y, Watanabe T, Asakawa S, Kimura M (2012b) Bacterial communities that decompose root cap cells in an anaerobic soil: estimation by DNA-SIP method using rice plant callus cells. Soil Sci Plant Nutr 58:297–308

Li JB, Rui JP, Pei ZJ, Sun XR, Zhang SH, Yan ZY, Wang YP, Liu XF, Zheng T, Li XZ (2014) Straw- and slurry-associated prokaryotic communities differ during co-fermentation of straw and swine manure. Appl Microbiol Biotechnol 98:4771–4780

Li HJ, Chang JL, Liu PF, Fu L, Ding DW, Lu YH (2015) Direct interspecies electron transfer accelerates syntrophic oxidation of butyrate in paddy soil enrichments. Environ Microbiol 17:1533–1547

Liesack W, Schnell S, Revsbech NP (2000) Microbiology of flooded rice paddies. FEMS Microbiol Rev 24:625–645

Luo F, Devine CE, Edwards EA (2016) Cultivating microbial dark matter in benzene-degrading methanogenic consortia. Environ Microbiol 18:2923–2936

Magoc T, Salzberg SL (2011) FLASH: fast length adjustment of short reads to improve genome assemblies. Bioinformatics 27:2957–2963

Martin M (2011) Cutadapt removes adapter sequences from high-throughput sequencing reads. EMBnet J 17:10–12

Millar N, Baggs EM (2005) Relationships between N_2O emissions and water-soluble C and N contents of agroforestry residues after their addition to soil. Soil Biol Biochem 37:605–608

Miron J, Ben-Ghedalia D (1992) The degradation and utilization of wheat-straw cell-wall monosaccharide components by defined ruminal cellulolytic bacteria. Appl Microbiol Biot 38:432–437

Moon YH, Iakiviak M, Bauer S, Mackie RI, Cann IKO (2011) Biochemical analyses of multiple endoxylanases from the rumen bacterium *Ruminococcus albus* 8 and their synergistic activities with accessory hemicellulose-degrading enzymes. Appl Environ Microb 77:5157–5169

Neufeld JD, Dumont MG, Vorha J, Murrell JC (2007) Methodological considerations for the use of stable isotope probing in microbial ecology. Microb Ecol 53:435–442

Nottingham AT, Hicks LC, Ccahuana AJ, Salinas N, Bååth E, Meir P (2018) Nutrient limitations to bacterial and fungal growth during cellulose decomposition in tropical forest soils. Biol Fertil Soils 54:219–228

Ozbayram EG, Kleinsteuber S, Nikolausz M, Ince B, Ince O (2017) Effect of bioaugmentation by cellulolytic bacteria enriched from sheep rumen on methane production from wheat straw. Anaerobe 46:122–130

Paul EA, Clark FE (1989) Soil microbiology and biochemistry. Academic Press, London, pp 93–97

Pérez J, Muñozdorado J, De lRT, Martínez J (2002) Biodegradation and biological treatments of cellulose, hemicellulose and lignin: an overview. Int Microbiol 5:53–63

Reichenbach H, Lang E, Schumann P, Spröer C (2006) *Byssovorax cruenta* gen. nov., sp. nov., nom. rev., a cellulose-degrading myxobacterium: rediscovery of '*Myxococcus cruentus*' Thaxter 1897. Int J Syst Evol Microbiol 56:2357–2363

Richmond PA (1991) Occurrence and functions of native cellulose. In: Haigler CH, Weimer JP (eds) Biosynthesis and biodegradation of cellulose. Dekker, New York, pp 5–23

Rotaru AE, Shrestha PM, Liu F, Markovaite B, Chen S, Nevin KP, Lovley DR (2014) Direct interspecies electron transfer between *Geobacter metallireducens* and *Methanosarcina barkeri*. Appl Environ Microb 80:4599–4605

Rui JP, Peng JJ, Lu YH (2009) Succession of bacterial populations during plant residue decomposition in rice field soil. Appl Environ Microb 75:4879–4886

Ruppel S, Torsvik V, Daae FL, Øvreås L, Rühlmann J (2007) Nitrogen availability decreases prokaryotic diversity in sandy soils. Biol Fertil Soils 43:449–459

Saiz-Jimenez C (1996) The chemical structure of humic substances: recent advances. In: Piccolo A (ed) Humic substances in terrestrial ecosystems. Elsevier, Amsterdam, pp 1–45

Schöler A, Jacquiod S, Vestergaard G, Schulz S, Schloter M (2017) Analysis of soil microbial communities based on amplicon sequencing of marker genes. Biol Fertil Soils 53:485–489

Seneviratne G (2000) Litter quality and nitrogen release in tropical agriculture: a synthesis. Biol Fertil Soils 31:60–64

Shan J, Yan XY (2013) Effects of crop residue returning on nitrous oxide emissions in agricultural soils. Atmos Environ 71:170–175

Shaw AK, Halpern AL, Beeson K, Tran B, Venter JC, Martiny JBH (2008) It's all relative: ranking the diversity of aquatic bacterial communities. Environ Microbiol 10:2200–2210

Shrestha PM, Rotaru AE, Summers ZM, Shrestha M, Liu F, Lovley DR (2013) Transcriptomic and genetic analysis of direct interspecies electron transfer. Appl Environ Microbiol 79:2397–2404

Smith SA, Hughes E, Coats ER, Brinkman CK, McDonald AG, Harper JR, Feris K, Newby D (2016) Toward sustainable dairy waste utilization: enhanced VFA and biogas synthesis via upcycling algal biomass cultured on waste effluent. J Chem Technol Biot 91:113–121

Sun W, Krumins V, Dong Y, Gao P, Ma C, Hu M, Li B, Xia B, He Z, Xiong S (2017) A combination of stable isotope probing, illumina sequencing, and co-occurrence network to investigate thermophilic acetate- and lactate-utilizing bacteria. Microb Ecol 75:113–122

Vestergaard G, Schulz S, Schöler A, Schloter M (2017) Making big data smart—how to use metagenomics to understand soil quality. Biol Fertil Soils 53:479–484

Wang Q, Garrity GM, Tiedje JM, Cole JR (2007) Naive Bayesian classifier for rapid assignment of rRNA sequences into the new bacterial taxonomy. Appl Environ Microb 73:5261–5267

Wartiainen I, Eriksson T, Zheng W, Rasmussen U (2008) Variation in the active diazotrophic community in rice paddy-*nifH* PCR-DGGE analysis of rhizosphere and bulk soil. Appl Soil Ecol 39:65–75

Wegner CE, Liesack W (2016) Microbial community dynamics during the early stages of plant polymer breakdown in paddy soil. Environ Microbiol 18:2825–2842

Xiang X, Huang Y, Madey G, Cabaniss S, Arthurs L, Maurice P (2010) Modeling the evolution of natural organic matter in the environment with an agent-based stochastic approach. Nat Resour Model 19:67–90

Yi W, You J, Zhu C, Wang B, Qu D (2013) Diversity, dynamic and abundance of Geobacteraceae species in paddy soil following slurry incubation. Eur J Soil Biol 56:11–18

Zgadzaj R, Garrido-Oter R, Jensen DB, Koprivova A, Schulze-Lefert P, Radutoiu S (2016) Root nodule symbiosis in *Lotus japonicus* drives the establishment of distinctive rhizosphere, root, and nodule bacterial communities. Proc Natl Acad Sci U S A 113:E7996–E8005

Zhuang L, Tang J, Wang YQ, Hu M, Zhou SG (2015) Conductive iron oxide minerals accelerate syntrophic cooperation in methanogenic benzoate degradation. J Hazard Mater 293:37–45